Reversible ferromagnetism in rutile TiO_2 single crystals induced by nickel impurities

Y. L. Zhao, M. Motapothula, N. L. Yakovlev, Z. Q. Liu, S. Dhar, A. Rusydi, Ariando, M. B. H. Breese, Q. Wang, and T. Venkatesan'

Citation: Appl. Phys. Lett. **101**, 142105 (2012); doi: 10.1063/1.4756799
View online: http://dx.doi.org/10.1063/1.4756799
View Table of Contents: http://aip.scitation.org/toc/apl/101/14
Published by the American Institute of Physics

Reversible ferromagnetism in rutile TiO_2 single crystals induced by nickel impurities

Y. L. Zhao,[1,2] M. Motapothula,[1,2] N. L. Yakovlev,[3] Z. Q. Liu,[1,2] S. Dhar,[1,4] A. Rusydi,[1,2,5] Ariando,[1,2] M. B. H. Breese,[1,2] Q. Wang,[1,6] and T. Venkatesan[1,2,4,a)]
[1]*NUSNNI-NanoCore, National University of Singapore, 117411 Singapore*
[2]*Department of Physics, National University of Singapore, 117542 Singapore*
[3]*Institute of Materials Research and Engineering, 117602 Singapore*
[4]*Department of Electrical and Computer Engineering, National University of Singapore, 117576 Singapore*
[5]*Singapore Synchrotron Light Source, National University of Singapore, 117603 Singapore*
[6]*Department of Materials Science and Engineering, National University of Singapore, 117576 Singapore*

(Received 23 July 2012; accepted 17 September 2012; published online 3 October 2012)

We report a Ni impurity induced reversible ferromagnetism and surface conduction in rutile TiO_2 crystals subjected to specific thermal annealing. For annealing in vacuum at 800 °C, a growing ferromagnetic signal is seen with time while for a similar annealing in air, the magnetism vanishes. The magnetism is concomitant with a surface conductivity which at low temperatures shows tunneling characteristics. Here, we show that Ni magnetic impurity (in TiO_2 crystals at <100 ppm) under vacuum annealing segregates to the surface over a 50 nm layer where the Ni concentration exceeds 10%–20% and drops with subsequent air annealing. © *2012 American Institute of Physics*. [http://dx.doi.org/10.1063/1.4756799]

Oxide based dilute magnetic semiconductor (DMS) has attracted considerable attention because of the discovery of above room temperature ferromagnetism, anomalous Hall effect, and its potential applications in spintronics.[1–9] Among various oxides, TiO_2 is one of the most explored host material and many types of dopants have been introduced into this host. Cobalt doped TiO_2 generated great interest for its above room temperature ferromagnetism, where in some cases it was discussed as magnetism originating from Cobalt clusters.[1,2,6,7] In contrast, non magnetic atom doped TiO_2 also can show ferromagnetism, where cationic vacancies or Ti^{3+} induced by oxygen vacancies were discussed as the reason.[10–12] As all of these experiments used oxide crystals as the substrate, it is crucial to first confirm that the substrate is magnetically inert. Yee *et al*. observed that ferromagnetism arose only from commercial single side polished substrates of Al_2O_3, $LaAlO_3$, $SrTiO_3$, TiO_2, and ZnO where they claimed that Fe ions from the unpolished side gave ferromagnetism.[13] They showed reversibility of this ferromagnetism by implementing vacuum and subsequent atmospheric annealing. However, the detailed physical explanations for those observations were lacking.

In the present study, double side polished single crystal rutile TiO_2 (001) substrates were obtained from three different vendors.[14] The pristine samples were paramagnetic in nature. However, by annealing them in a vacuum environment, ferromagnetic property arises and it disappears with subsequent annealing in air, i.e., the phenomenon is reversible. As received and air annealed samples show insulating behavior while vacuum annealed sample is conductive at room temperature, where the metallic behavior is maintained until about 40 K. Secondary ion mass spectroscopy (SIMS), Rutherford back scattering (RBS), and high resolution transmission electron microscopy (HRTEM) equipped with energy dispersive x-ray (EDX) spectroscopy were used to analyze the origin of the magnetism and the conduction.

TiO_2 samples ($5 \times 5 \times 0.5$ mm^3) are annealed in high vacuum environment at 5×10^{-6} Torr at 800 °C. The transparent pristine sample becomes dark, which has been attributed to oxygen vacancies and some other defects,[15] as shown in Fig. 1(a) and turns into a pale yellow color by subsequent air annealing in a furnace. This process is highly repeatable. As received TiO_2 substrate shows paramagnetic property. After vacuum annealing for 2 h (heating and cooling rates are 10 K/min, where this time was not considered), a ferromagnetic loop is seen in the superconducting quantum interference device (SQUID) measurements at 10 K to 300 K. A subsequent air annealing for 2 h turns the samples back to the paramagnetic state, and when the sample is annealed in vacuum again under the same condition, ferromagnetism returns and becomes even stronger. The time dependence of the vacuum annealing of the substrates was studied and is shown in Fig. 1(b). By keeping the annealing temperature and pressure the same as in Fig. 1(a), it can be seen that the saturation magnetic moment (M_s) continuously increases with annealing time; however, the coercivity (H_c) remains constant. Temperature dependent vacuum annealing of the substrates is shown in Fig. 1(c), where it can be seen that below 600 °C ferromagnetism cannot be turned on for the duration of time studied (2 h). This temperature corresponds to 75 meV of thermal energy. In plane and out plane magnetic moments (M) to magnetic field (H) relation curve were plotted in Fig. 1(d), where the sample was annealed in vacuum for 4 h and with temperature and pressure the same as in Fig. 1(a). By considering only the in-plane MH loop at different temperatures, it can be found that both M_s and H_c decrease with increasing measurement temperature. And it is similar for the out of plane case, where at room temperature, H_c disappears, as shown in the inset of Fig. 1(d). Generally, the M_s measured in plane is much larger than that

a)Electronic mail: venky@nus.edu.sg.

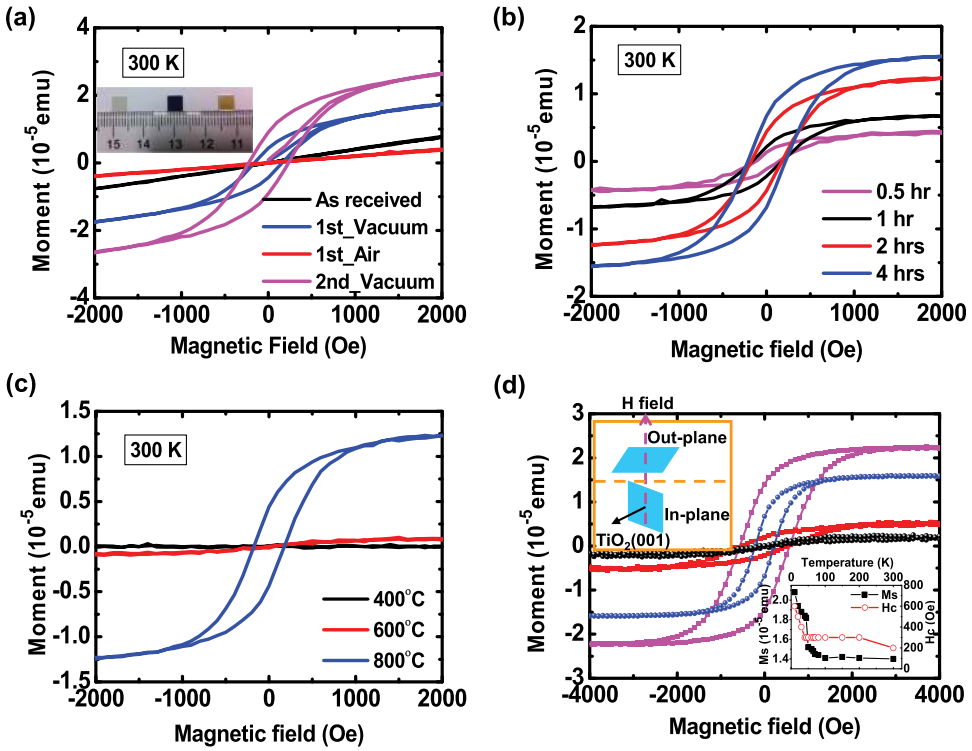

FIG. 1. (a) Magnetic moment versus field (MH) measurement of TiO_2 substrate at room temperature. The annealing temperature is 800 °C and the annealing time is 2 h. The vacuum level is kept at 5×10^{-6} Torr. Inset shows the photo of pristine, vacuum annealed, and subsequently air annealed samples. (b) Room temperature MH measurements of TiO_2 substrates vacuum annealed with 800 °C for different times. Here, paramagnetic part of the signal was deducted. (c) Room temperature MH measurements of TiO_2 substrates vacuum annealed for 2 h with different temperatures. Only the ferromagnetism component is shown. (d) MH measurement at 10 K and room temperature of samples oriented in plane and out of plane with magnetic field. Black and red colors indicate the out of plane plot at room temperature and 10 K. Blue and fuchsia colors indicate the in plane plot at room temperature and 10 K, respectively. Inset at the left corner shows the schematic graph of in plane and out of plane configuration. Inset at the right corner shows the changes of saturation magnetization and coercivity with temperature in the in plane measurement.

measured out of plane. This indicates strong anisotropy of the ferromagnetism.

Temperature dependent resistivity (ρ-T) of TiO_2 crystals annealed 2, 4, and 8 h in vacuum are measured in the temperature range of 20 to 400 K, as shown in Fig. 2(a), where in this plot, two transitions can be observed around 40 and 280 K. Above 280 K, the resistivity decreases slowly with increasing temperature. Below 40 K, the decrease of resistivity with increasing temperature becomes more dramatic. In between 40 and 280 K, metallic behavior can be seen, where closer to 40 K regimes, resistivity changes much faster than that closer to 280 K regimes. The charge carrier density and the mobility between 20 and 360 K are plotted in Fig. 2(b). The charge carrier density increases with temperature until 40 K and then decreases with temperature until 100 K, after which, it shows increasing behavior again. In contrast, the mobility increases sharply with temperature between 20 and 40 K and then decreases continuously. The differences in the resistivity, carrier density, and mobility for the samples annealed in vacuum for different times (2, 4, and 8 h) are relatively small.

To understand the nature of the above magnetic and electronic phenomena, the purity of the substrates was first checked by SIMS using calibrated standards as reference (TiO_2 thin films containing 1% Ni, 1% Fe, 1% Co, 1% Mn, and 1% Cr on Si substrate). Ni is the dominant magnetic impurity at 100 ppm level in the as received sample. In contrast, the concentrations of other standard magnetic impurities are at least one to two orders of magnitude smaller. As shown in Fig. 3(a), around 10% Ni was observed in the sample after vacuum annealing with 800 °C for 4 h. Even after air annealing, around 1% Ni still can be detected. Hence one can speculate that the ferromagnetism of TiO_2 substrate comes dominantly from Ni impurities though more evidence is

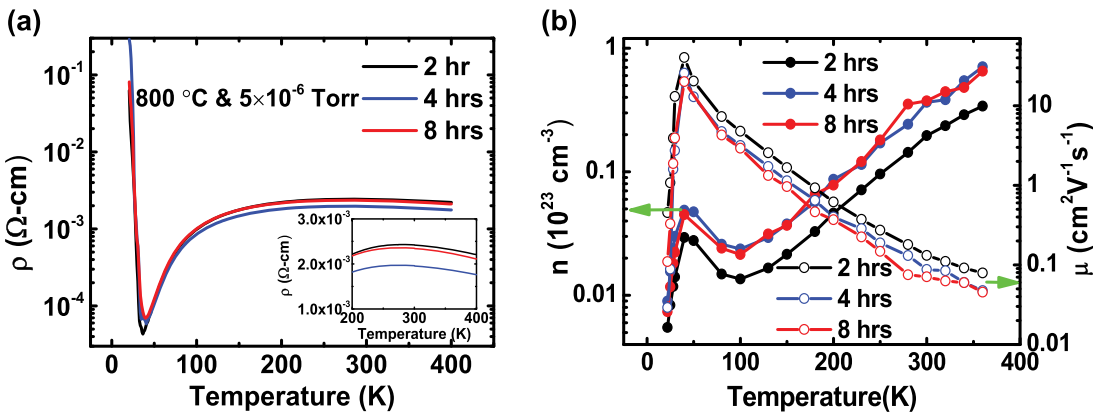

FIG. 2. (a) Temperature dependent resistivity measurement of TiO_2 samples vacuum annealed for 2, 4, and 8 h. Thickness of 50 nm was used in the calculation. The curve near 300 K is expanded in the inset. (b) Hall effect measurement of the samples described in (a). The solid circles indicate the charge carrier density and the open circles represent mobility.

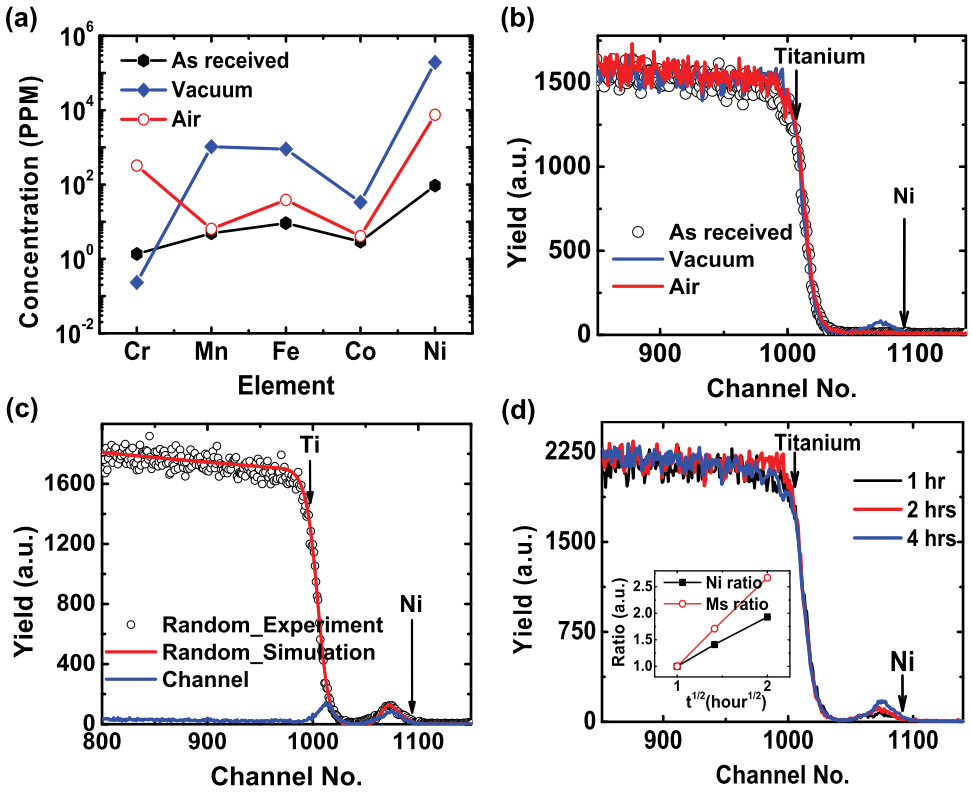

FIG. 3. (a) SIMS data of as received, vacuum annealed, and air annealed TiO_2. The vacuum and air annealing time is 4 h. (b) RBS random curve of as received, vacuum annealed, and air annealed TiO_2 substrates as in (a). (c) RBS random, channeling, and curve fit for the vacuum annealed sample in (a). (d) RBS random peak of TiO_2 samples vacuum annealed for 1, 2, and 4 h. Inset shows Ni peak intensity ratio and M_s ratio of the TiO_2 samples annealed in vacuum for different times. Ni peak intensity was calculated by integration of the Ni peak area.

required to substantiate the claim. RBS was done in order to verify this argument. As shown in Fig. 3(b), in both as received and air annealed samples, Ni concentration was too low to be detected. However, in the vacuum annealed sample, a significant Ni peak can be seen. The Ni concentration is around 12% out of 100% Ti by considering the peak to peak values in the 4 h vacuum annealed substrate, which is close to the value obtained by SIMS. As shown in Fig. 3(c), the RBS spectrum of vacuum annealed samples can be well fitted by Gaussian distribution, and the RBS random and channeled peaks of Ni overlap each other, which indicate that all the Ni atoms are in the interstitial locations. In addition, the surface peak of Ti is also quite large, which means that there is crystalline disorder near the surface. The concentration of Ni in TiO_2 substrates which were vacuum annealed for 1, 2, and 4 h was measured by RBS, as shown in Fig. 3(d). The intensity of the Ni peak increases with annealing time, which is consistent with the increasing behavior of the ferromagnetism. Interestingly, the Ni peaks are almost centered at the same position. The integrated Ni intensity ratio from RBS was plotted in the inset of Fig. 3(d), where the M_s ratio of those samples was shown as well. Both Ni intensity and the M_s increase with vacuum annealing time (t) as $t^{1/2}$ suggesting a diffusion process. As can be seen, the M_s ratio increases faster than Ni intensity ratio, which suggests nonlinear ferromagnetic coupling with increasing Ni concentration. From thermodynamic point of view, the formation of Ni clusters is preferable under oxygen poor condition. As the bonding energy of Ni-O (373 ± 3 kJ/mol) is smaller than Ti-O (672.4 ± 9.2 kJ/mol),[16,17] when oxygen escapes from TiO_2 due to vacuum annealing, Ti is more competitive with respect to Ni in forming bond with the left over oxygen. Hence Ni forms metallic clusters near the surface.

TEM equipped with EDX shows the existence of Ni clusters near the sample surface as well. As shown in Fig. 4(a), a HRTEM cross sectional image of the 4 h vacuum annealed TiO_2 sample is seen. In Fig. 4(b), an element sensitive EDX scan of the same region is shown where it is seen that Ni is distributed densely within a 50 nm region close to the sample surface. As suggested by RBS channeling data, Ni may exist as interstitials or clusters. A higher resolution image shows such granular regions in the inset of Fig. 4(a). The granular Ni clusters in the ~50 nm TiO_2 surface layer may partly explain the transport behavior as well. If we assume that all the electrons from room temperature to 40 K were contributed by Ni atoms spread within a 50 nm region near the sample surface, it can be deduced from Fig. 2(b) that the Ni concentration is about 10% in that region, which is a reasonable value. (If we assume a Gaussian distribution the Ni density near the center of this region may be closer to 30% or more providing near percolation.)[18] Of course, Ti interstitials may contribute electrons as well.[19] Because Ni does not form a continuous sheet, rather clusters with a small separation (tunnel barriers), the transport is similar to a cermet structure. This explains the relatively flat resistivity from room temperature to 40 K with a value close to 10^{-3} Ω·cm, characteristic of a bad metal. At very low temperatures, the tunnel barrier causes the resistivity to diverge and the barrier energy is about 3.4 meV.

Ni contribution to ferromagnetism in TiO_2 substrate was reported before,[20] where Ni ions were intentionally ion implanted into TiO_2 crystal and the relationship of ferromagnetism with Ni concentration was studied. However, in that work, one observation could not be explained properly. The measured saturation magnetization was much larger than the expected value of $0.61\mu_B$/Ni. Hence current experimental result has given an answer to this controversy. In their case

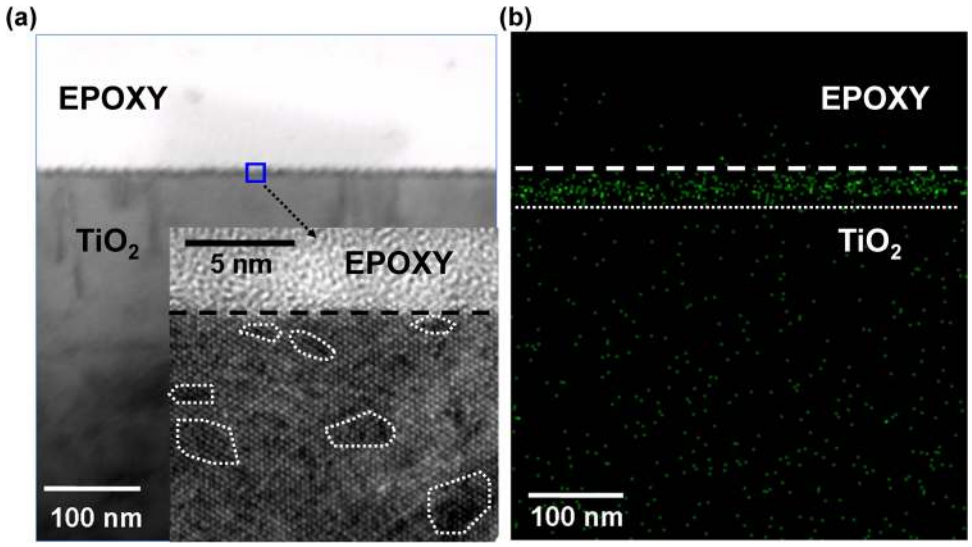

FIG. 4. (a) HRTEM image of TiO_2 crystal vacuum annealed at 800 °C for 4 h. The likely Ni rich areas are shown by white circles. (b) Elemental scan of the same area described in (a), where the two dashed lines show the boundary of the Ni rich region.

clearly in addition to the ion implanted Ni, there was impurity Ni dissolved in the substrate which segregated during the implantation annealing process adding to the Ni concentration at the surface.

In summary, vacuum annealed rutile TiO_2 crystal shows ferromagnetism, and we show that the magnetic source is Ni clusters segregated by Ni contaminants that exist as NiO at 100 ppm level in commercially available TiO_2 substrates. The segregation is thermally activated with a 75 meV barrier and under vacuum annealing, causes Ni to accumulate at the top surface and under subsequent air annealing Ni redissolves into the bulk. This segregated surface layer of Ni gives rise to the observed ferromagnetism and the surface conductance. The cermet structure of this layer leads to a bad metal which exhibits a tunneling behavior at low temperatures. Researchers in the field of DMS oxides are hence cautioned to not only check the level of magnetic impurities in the as received substrates (not limited to TiO_2, but also applied to others like $SrTiO_3$, ZnO, Al_2O_3, etc.) but also to double check the properties of the substrates under the film preparation conditions to minimize substrate interference in the film data.

The authors appreciate the discussions with Huang Zhen, Qi Dongchen, and Ou Hongwei. This work was supported by NUSNNI-Nanocore start-up grant, NRF-CRP grants "Tailoring Oxide Electronics by Atomic Control" (NRF2008NRF-CRP002-024) and MOE-AcRF-Tier-2.

[1]Y. Matsumoto, M. Murakami, T. Shono, T. Hasegawa, T. Fukumura, M. Kawasaki, P. Ahmet, T. Chikyow, S. Koshihara, and H. Koimuma, Science **291**, 854 (2001).
[2]S. R. Shinde, S. B. Ogale, S. Das Sarma, J. R. Simpson, H. D. Drew, S. E. Lofland, C. Lanci, J. P. Buban, N. D. Browning, V. N. Kulkarni, J. Higgins, R. P. Sharma, R. L. Greene, and T. Venkatesan, Phys. Rev. B **67**, 115211 (2003).
[3]S. B. Ogale, R. J. Choudhary, J. P. Buban, S. E. Lofland, S. R. Shinde, S. N. Kale, V. N. Kulkarni, J. Higgins, C. Lanci, J. R. Simpson, N. D. Browning, S. Das Sarma, H. D. Drew, R. L. Greene, and T. Venkatesan, Phys. Rev. Lett. **91**, 077205 (2003).
[4]S. N. Kale, S. B. Ogale, S. R. Shinde, M. Sahasrabuddhe, V. N. Kulkarni, R. L. Greene, and T. Venkatesan, Appl. Phys. Lett. **82**, 2100 (2003).
[5]D. C. Kundaliya, S. B. Ogale, S. E. Lofland, S. Dhar, C. J. Metting, S. R. Shinde, Z. Ma, B. Varughese, K. V. Ramanujachary, L. Salamanca Riba, and T. Venkatesan, Nature Mater. **3**, 709 (2004).
[6]S. R. Shinde, S. B. Ogale, J. S. Higgins, H. Zheng, A. J. Millis, V. N. Kulkarni, R. Ramesh, R. L. Greene, and T. Venkatesan, Phys. Rev. Lett. **92**, 166601 (2004).
[7]S. X. Zhang, W. Yu, S. B. Shinde, D. C. Kundaliya, W.-K. Tse, S. Y. Young, J. S. Higgins, L. G. Salamanca-Riba, M. Herrera, L. F. Fu, N. D. Browing, R. L. Greene, and T. Venkatesan, Phys. Rev. B **76**, 085323 (2007).
[8]L. F. Fu, N. D. Browning, S. X. Zhang, S. B. Ogale, D. C. Kundaliya, and T. Venkatesan, J. Appl. Phys. **100**, 123910 (2006).
[9]T. S. Herng, D.-C. Qi, T. Berlijn, J. B. Yi, K. S. Yang, Y. Dai, Y. P. Feng, I. Santoso, C. Sánchez-Hanke, X. Y. Gao, A. T. S. Wee, W. Ku, J. Ding, and A. Rusydi, Phys. Rev. Lett. **105**, 207201 (2010).
[10]S. Duhalde, M. F. Vignolo, F. Golmar, C. Chiliotte, C. E. Rodríguez Torres, L. A. Errico, A. F. Cabrera, M. Rentería, F. H. Sánchez, and M. Weissmann, Phys. Rev. B **72**, 161313 (2005).
[11]J. Osorio-Guillén, S. Lany, and A. Zunger, Phys. Rev. Lett **100**, 036601 (2008).
[12]A. Roy Barman, A. Annadi, K. Gopinadhan, W. M. Lu, Ariando, S. Dhar, T. Venkatesan, AIP Adv. **2**, 012148 (2012); A. Rusydi, S. Dhar, A. Roy Barman, Ariando, D.-C. Qi, M. Motapothula, J. B. Yi, I. Santoso, Y. P. Feng, K. Yang, Y. Dai, N. L. Yakovlev, J. Ding, A. T. S. Wee, G. Neuber, M. B. H. Breese, M. Ruebhausen, H. Hilgenkamp, and T. Venkatesan, Phil. Trans. R. Soc. A **370**, 4927 (2012).
[13]S. M. M. Yee, D. A. Crandles, and L. V. Goncharova, J. Appl. Phys. **110**, 033906 (2011).
[14]CrysTec GmbH Kristalltechnologie, Germany; MTI Corporation, USA; Shinkosha Co., Ltd, Japan.
[15]U. Diebold, Surf. Sci. Rep. **48**, 53–229 (2003).
[16]L. R. Watson, T. L. Thiem, R. A. Dressler, R. H. Salter, and E. Murad, J. Phys. Chem. **97**, 5577 (1993).
[17]K. De Buysser, I. Van Driessche, B. V. Putte, P. Vanhee, J. Schaubroeck, and S. Hoste, Inorg. Chem. **47**, 736 (2008).
[18]S. Kirkpatrick, Rev. Mod. Phys. **45**, 574 (1973).
[19]E. Yagi, R. R. Hasiguti, and M. Aono, Phys. Rev. B **54**, 7945 (1996).
[20]B. F. Ding, Y. P. Li, and L. M. Wang, Chin. Phys. Lett. **28**, 107802 (2011).